# Fracture Control in Composite Materials Using Integral Crack Arresters

T. E. Hess,* S. L. Huang,† and H. Rubin‡
*Naval Air Development Center, Warminster, Pa.*

**Damage tolerance and survivability have become important design criteria for future military aircraft structures. The inherent flaws which exist in a structural material or the damage sustained in combat, if uncontrolled, can grow to critical sizes and lead to failure of a component or, possibly, the entire aircraft. The objective of this study has been to investigate and develop crack arrester designs for composite materials which will contain cracks and damage locally, thereby allowing an aircraft and crew to return safely to base for repair or replacement of damaged parts. This is accomplished by using crack arrester strips which form a barrier and prevent a crack from propagating beyond them. This paper presents the results obtained in the first phase of these studies, in which it has been shown that crack arrester strips do stop and contain the damage, and that the use of these strips will provide survivability at significantly less weight than designs in which survivability is achieved by limiting the operating strain. These conclusions are based on both analysis and tests performed on specimens of variable thickness, size, and laminate configuration in which failure modes and critical conditions have been characterized.**

## Introduction

STUDIES have been underway at the Naval Air Development Center for two years on the use of crack arrester strips in advanced composite materials as a means of stopping a propagating crack and limiting the damage which is induced in the structure. A goal of these studies has been to give a structure the ability to carry limit load after sustaining the damage, thereby allowing it to make a safe return to base for repair or replacement of the damaged part. At the start of these studies, analysis and testing were performed to verify that a rapidly propagating crack could be arrested by these strips. Very quickly the feasibility of the concept was demonstrated, and work continued to investigate further its behavior and to develop a limited data base which could be used to evaluate applications to actual aircraft designs. At the same time, it was decided to incorporate crack arrester strips into the design of a low-cost hybrid fuselage prototype to meet the goal of increased survivability for that component.[1] Additional work has now been done to characterize more completely the initial crack propagation and residual strength of graphite-epoxy composites containing crack arrester strips.

This latest work completes the first phase of the study of crack arrester strip designs. It is the intent of this paper to present the results obtained to date and set the perspective for future activity in this area.

## Materials and Laminate Configuration

The work presented in this paper, including the test results, is based on use of graphite-epoxy material with a generic layup of $[0°/\pm 45°/0°]_{ns}$. Hercules AS/3501 graphite-epoxy has been used throughout except for four of the early test specimens which were fabricated with Narmco 5209 Type II graphite-epoxy. In all of the cases the crack arrester strips have been parallel strips formed by replacing the 0° graphite-epoxy with 0° glass-epoxy over the width of the strip. Two types of 3M glass-epoxy have been used: Scotchply SP-250-SF-1 S-glass and XP-114 E-glass, with no significant difference in the results obtained.

## Design and Failure Modes

In order to lay the theoretical groundwork for behavior of the crack arrester strips, the analysis of initial crack propagation and propagation across the arrester strip is presented here, based on Ref. 2. The critical stress at which an existing crack will propagate is

$$\sigma_{cr} = K_Q / [\pi(c+a)]^{1/2} \tag{1}$$

where

$K_Q$ = fracture toughness
$a$ = characteristic dimension of intense energy region
$2c$ = crack length

$K_Q$ and $a$ are determined from two tests, one on a specimen with a crack and one on an uncracked control specimen. From these tests

$$a = c/[(\sigma_\infty/\sigma_{cr})^2 - 1] \tag{2}$$

$$K_Q = \sigma_\infty (\pi a)^{1/2} \tag{3}$$

where

$\sigma_{cr}$ = applied failure stress for specimen with crack
$\sigma_\infty$ = failure stress of uncracked specimen

The function of the crack arrester strip is to provide a low-stress, high-toughness region which will render a crack entering this region noncritical. In order for a crack to be arrested and the structure to continue to carry limit load, the following condition, which is derived from Eq. (1), must be met:

$$\sigma_{cr_2} = \frac{K_{Q2}}{[\pi(W_1/2 + a_2)]^{1/2}} \geq \frac{E_2}{E_1}\sigma_{1_{\lim}} \tag{4}$$

$E$ is modulus of elasticity and $w_1$ is material width. As shown in Fig. 1, the 1 subscripts refer to the primary material and the 2 subscripts to the crack arrester strip.

Presented at the AIAA/ASME/SAE 17th Structures, Structural Dynamics, and Materials Conference, King of Prussia, Pa., May 5-7, 1976 (in bound volume of Conference papers, no paper number); submitted May 20, 1976; revision received April 11, 1977.

Index categories: Structural Composite Materials; Structural Design.

*Head, Design and Analysis Section, Structures Research and Development Branch.

†Head, Structures Research and Development Branch, Structures Division.

‡Aerospace Engineer, Structures Research and Development Branch.

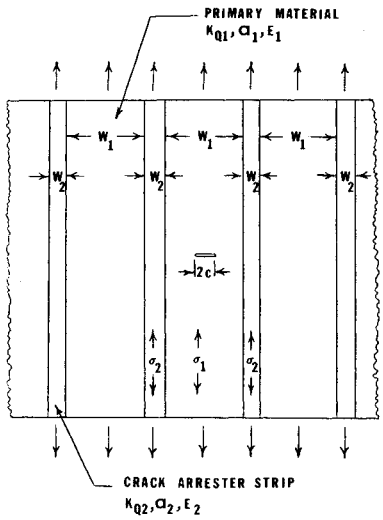


**Fig. 1 Nomenclature for crack arrester design.**

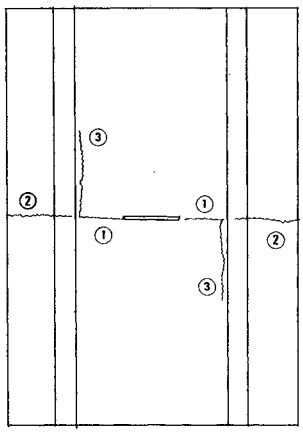


**Fig. 2 Failure modes in crack arrester strip design.**

A finite width correction factor is used as given in Eq. (5), which is taken from Ref. 3.

$$f\left(\frac{c}{W_1}\right) = \frac{1}{[1-(2c/w_1)^2]^{1/2}} \tag{5}$$

Using this correction factor, Eq. (1) becomes

$$\sigma_{cr} = \frac{K_Q[1-(2c/w_1)^2]^{1/2}}{[\pi(c+a)]^{1/2}} \tag{6}$$

Besides these two failure modes, initial crack propagation and propagation across the arrester strips, a third failure mode exists – that of shear failure along the boundary between the cracked primary material and the crack arrester strip. All three of these are depicted in Fig. 2. It is the third failure mode that has been found in this study to be the one which determines the residual strength of a panel with an arrested crack. Analytical treatment of this failure mode is somewhat of a more difficult task. In this study two-dimensional finite-element techniques have been used.

## Analysis and Tests

Most of the testing performed in the study of crack arrester strip designs was done with small single-bay panels. These panels were 6 in. wide, 9 in. long, and contained two crack arrester strips. Later, it became necessary to fabricate and test larger panels containing several crack arrester strips, i.e., multibay panels. Table 1 gives a description of all of the specimens in terms of thickness, crack size, and materials

**Table 1 Single-bay and multibay panel test specimens**

| Panel no. | $t_1$,[a] in. | $t_2$,[b] in. | $w_1$, in. | Initial crack length, in. | Primary material | Crack arrester material[c] |
|---|---|---|---|---|---|---|
| | | | | Single-bay | | |
| S1 | 0.06 | 0.06 | 2 | 0.24 | N[d] | SP[f] |
| S2 | 0.06 | 0.06 | 3 | 0.22 | | |
| S3 | 0.06 | 0.06 | 3 | 0.14 | | |
| S4 | 0.06 | 0.06 | 3 | 0.20 | | |
| S5 | 0.16 | 0.17 | 3 | 0.20 | H[e] | |
| S6 | 0.16 | 0.17 | 3 | 0.08 | | |
| S7 | 0.16 | 0.17 | 3 | 0.75 | | |
| S8 | 0.25 | 0.26 | 3 | 0.50 | | |
| S9 | 0.38 | 0.47 | 3 | 0.75 | | |
| S10 | 0.38 | 0.47 | 3 | 0.30 | | |
| | | | | Multibay | | |
| M1 | 0.15 | 0.15 | 3 | 2.00/4.00 | H[e] | XP[g] |
| M2 | 0.14 | 0.14 | 3 | 2.00 | | |
| M3 | 0.10 | 0.10 | 6 | 3.00 | | |

[a] $t_1$ = primary material thickness.
[b] $t_2$ = crack arrester strip thickness.
[c] material for 0° plies in crack arrester strip.
[d] NARMCO 5209 Type II, graphite-epoxy.
[e] Hercules AS/3501, graphite-epoxy.
[f] Scotchply SP-250-SF1, glass-epoxy (S-glass), by 3M Co.
[g] XP-114, glass-epoxy (E-glass), by 3M Co.

used. Note that the crack arrester strip was thicker than the primary material in specimens S5 through S10 because of the greater per-ply thickness of the SP-250-SF1. However, a new glass-epoxy prepreg, XP114, was obtained and used in the fabrication of the multibay specimens. This material has the same basic per-ply thickness as the graphite-epoxy so the arrester strip thickness buildup, which was experienced in the earlier panels, was eliminated. The first panel had a 1-in. wide crack arrester strips 2-in. apart. In all of the other panels the crack arrester strips were ½-in. wide, spaced as indicated in Table 1. Note that spacing here, and in other parts of this paper, is defined as the distance between the strips, $w_1$ in Fig. 1, not center-to-center spacing.

Each of these panels was tested to the point of initial crack propagation and then to complete failure. In some cases this happened essentially simultaneously, since the load at initial propagation was high enough to induce ultimate failure. For most of the specimens, coupons made in the same cure cycle were tested in tension to determine modulus and strength, and in short beam shear to determine interlaminar shear strength. Test results are presented in terms of the global or gross strain using the measured modulus for the particular specimen.

Tables 2 and 3 give a summary of the test data for the ten single-bay and three multibay specimens. The values of initial propagation and residual strain were calculated based on the test load and the panel gross cross-section stiffness, using measured material thicknesses and measured modulus. The initial propagation strain was multiplied by the finite width correction factor from Eq. (5) to obtain the values of corrected initial propagation strain. No such correction was applied to residual strain. Note also that two tests were able to be run on panel M1 because of its having five bays, hence, the two sets of results for it in Table 3. These results also are plotted in Fig. 3 in terms of gross strain vs damage size. For the case of residual strength, damage size is the size of the arrested damage, which is equal to the crack arrester strip spacing. The curve shown for initial propagation represents a lower bound of the test data. It is somewhat higher than had been predicted using Eq. (6) together with early characterization data on graphite-epoxy of this layup configuration. No explanation of this is offered except to say that modulus was not measured on the material used for that characterization, and therefore, an analytical value of modulus had to be used for calculating predicted strain. Figure 4 shows a

**Table 2 Single-bay panel test results**

| Panel no. | $t_1$,[a] in. | Initial crack length, in. | Primary material modulus, MSI | Initial propagation strain, $\mu$ in./in. | Finite width correction | Corrected initial propagation strain, $\mu$ in./in. | Residual strain, $\mu$ in./in. |
|---|---|---|---|---|---|---|---|
| S1 | 0.06 | 0.24 | 10.9[b] | 4200 | 1.007 | 4230 | 5780 |
| S2 | 0.06 | 0.22 | 10.9[b] | 4310 | 1.003 | 4320 | ... |
| S3 | 0.06 | 0.14 | 10.9[b] | 5000 | 1.001 | 5000 | 5000[c] |
| S4 | 0.06 | 0.20 | 10.9[b] | 5100 | 1.002 | 5110 | 5100[c] |
| S5 | 0.16 | 0.20 | 10.9 | 4570 | 1.002 | 4580 | 4310 |
| S6 | 0.16 | 0.08 | 10.9 | 5620 | 1.000 | 5620 | 5620[c] |
| S7 | 0.16 | 0.75 | 10.9 | 3260 | 1.033 | 3370 | 4150 |
| S8 | 0.25 | 0.50 | 10.9[b] | 3700 | 1.014 | 3750 | 4110 |
| S9 | 0.38 | 0.75 | 10.9[b] | 3280 | 1.033 | 3390 | 4080 |
| S10 | 0.38 | 0.30 | 10.9[b] | 4360 | 1.005 | 4380 | 4360[c] |

[a] $t_1$ = primary material thickness.
[b] Modulus assumed to be same as measured for panels S5, S6, and S7.
[c] Ultimate failure simultaneous with initial crack propagation.

**Table 3 Multibay panel test results**

| Panel no. | $t_1$,[a] in. | Initial crack length, in. | Primary material modulus, MSI | Initial propagation strain, $\mu$ in./in. | Finite width correction | Corrected initial propagation strain, $\mu$ in./in. | Residual strain, $\mu$ in./in. |
|---|---|---|---|---|---|---|---|
| M1 (5-bay) | 0.15 | 2.00 | 10.6 | 1780 | 1.342 | 2390 | ...[b] |
| | | 4.00 | 10.6 | 1490 | 1.269 | 1890 | ...[b] |
| M2 (3-bay) | 0.14 | 2.00 | 11.7 | 1720 | 1.342 | 2310 | 4970 |
| M3 (3-bay) | 0.10 | 3.00 | 11.6 | 2240 | 1.155 | 2590 | 3550 |

[a] $t_1$ = primary material thickness.
[b] Residual strength results were invalid due to a premature failure away from the crack.

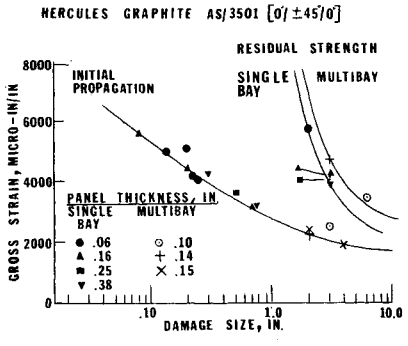


**Fig. 3 Critical strain for initial crack propagation and residual strength.**

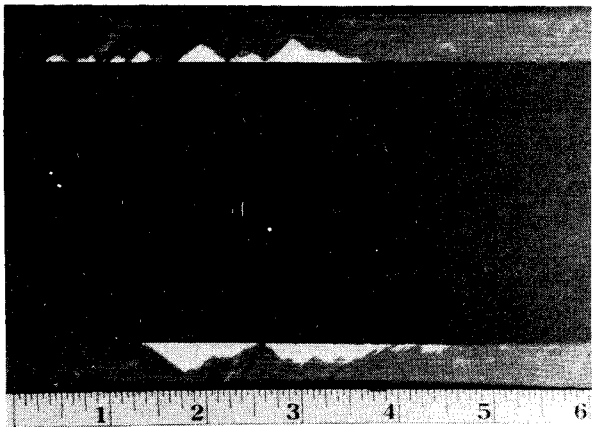


**Fig. 4 Initial crack propagation and arrestment.**

typical arrested crack in a single-bay graphite-epoxy panel. A multibay panel after initial propagation is shown in Fig. 5.

Examination of the initial propagation results on Fig. 3 indicates certain characteristics of this behavior. First of all, the relationship between propagation strain and damage size is well behaved with not too much scatter. One of the things being looked for in these tests was a possible thickness effect, and it is seen that there is none in the range considered here, from 0.06-0.38 in. It also is seen that the data tend to level off at the larger crack sizes, and, for purposes of the tradeoff analysis discussed later in this paper, it was assumed that this leveling off is at a strain value of 1700 $\mu$ in./in. It also appears that the multibay panel data fit in well with the single-bay data, and on this basis it was concluded that panel size had no significant effect on the results for initial propagation.

Interpretation of the results of the residual strength tests requires more discussion in view of the nature of the failure mode. In all of the cases, final failure of the specimen was in the form of shear along the arrester strip boundary as previously discussed and shown in Fig. 6 for a single-bay panel. A continuation of the crack propagation across the arrester strip was not experienced in any of the tests. The residual strength curve in Fig. 3 for the small single-bay panels is similar to the initial crack propagation curve in that it is a lower bound curve through the test data. The shape of the curve was determined by a simple hand analysis which attempted to determine the maximum shear stress as a function of crack arrester strip spacing. Note that the residual strength data points from Table 2 for specimens S3, S4, S6, and S10, which experienced ultimate failure simultaneously with initial propagation, are not plotted, since these do not represent a failure threshold. For these specimens the strain which existed at initial crack propagation was in excess of that

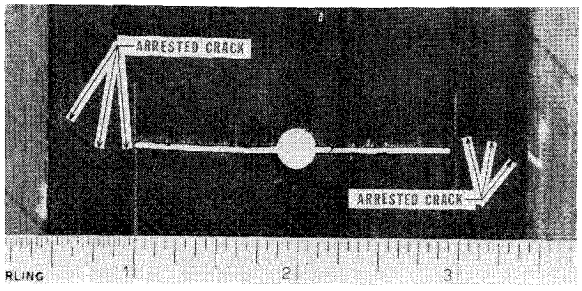


Fig. 5 Crack arrestment in multibay panel.

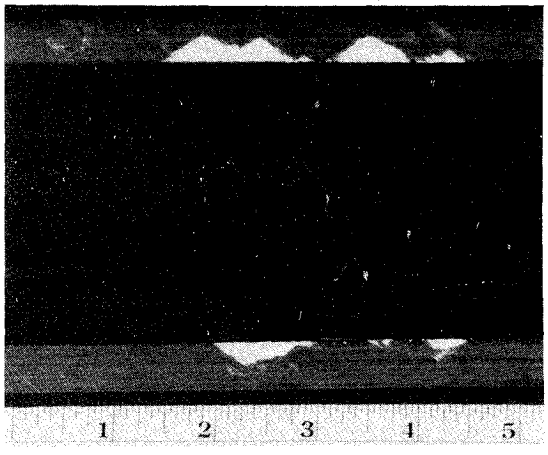


Fig. 6 Residual strength shear failure.

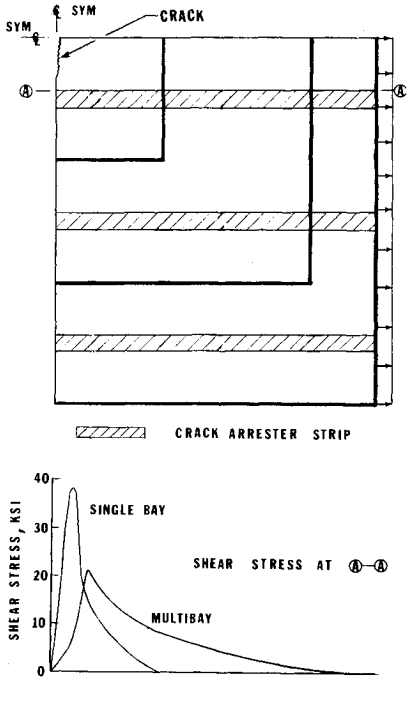


Fig. 7 Finite-element analysis.




required to cause ultimate failure, but by some unknown amount.

In order to understand better the nature of the residual strength and the factors affecting the shear failure mode, finite-element analyses of panels with an arrested crack were performed. Three panel sizes, as indicated by the heavy lines in Fig. 7, were analyzed to evaluate the effect of length and width on the maximum shear stress. The main conclusions from this analysis are as follows. In a specimen with three bays the shear stress is significantly less than in one with a single bay. However, the addition of two more bays, for a total of five, shows no further improvement over the results for three bays. In fact, the results were so close as to be almost indistinguishable in plotting, hence, the one curve in Fig. 7 labeled "multibay." So it would seem that the important thing is to provide at least one bay on either side of the damaged bay for load redistribution. Shear stress distributions along the arrester strip adjacent to the arrested crack are shown in Fig. 7 for a single-bay and multibay configuration. Length of the panel had no appreciable effect on the maximum shear stress. For the multibay panel the maximum shear stress is 45% less than in the single-bay panel, and so it would be expected that the residual strength of the multibay specimen would be 80% greater than the single bay. Verification of this increased residual strength was the major motivation for the multibay panel tests, since these are more representative of an actual aircraft structure than a single-bay specimen.

Two data points for residual strength of multibay panels have been obtained, one from specimen M2 which was a three-bay panel with crack arrester strips 3 in. apart, and one from specimen M3, also a three-bay specimen but with 6-in.-spaced crack arrester strips.

In panel M2 shear failure occurred at a strain of 4970 $\mu$ in./in. This was 25% higher than the lower bound data for the single-bay specimens, compared to the 80% increase predicted from analysis. Based on this first test, therefore, the curve for residual strength of multibay panels shown in Fig. 3 was drawn reflecting a 25% higher value of gross strain than the single-bay panels.

Specimen M3, with arrester strips 6 in. apart, represented the first test of a panel with crack arrester strip spacing greater than 3 in. Its residual strength shear failure occurred at a strain of 3550 $\mu$ in./in. This value was somewhat higher than expected based upon the "25% increase" curve which was drawn for multibay panels. Although more data are required fully to characterize the multibay panel behavior, the main conclusion from these limited results is that the residual strength of actual aircraft structures is significantly greater than that indicated by small single-bay panels.

## Design Tradeoffs

The use of integral crack arrester strips, such as those which are being discussed in this paper, can give an aircraft structural component improved damage survivability, but, in order to be as objective as possible, other alternatives must be considered. The most obvious alternative is simply to limit the level of strain in the component, a wing skin for example, by making it thicker so that sufficient inherent resistance to damage exists. Using the initial propagation curve of Fig. 3 it can be seen that, if the strain is kept below 1700 $\mu$ in./in., the structure can accommodate any reasonable damage size without further propagation. However, the weight implications of these approaches must be examined and some consideration given to their comparative costs.

The tradeoff analysis presented here is based on the criteria that, after sustaining damage, the structure should be capable of carrying limit strain, that is, two-thirds of its design ultimate strain. A comparison was made of the requirements of the two design approaches for satisfying this condition. In making these comparisons, design ultimate strain sometimes is used as an independent variable. It is assumed here that design conditions or criteria other than damage survivability establish this value. For ease of presenting the results, thicknesses and weight associated with designs which used crack arrester strips are referred to by using a subscript "*CAS*." Thicknesses and weights for designs in which survivability is achieved by controlling the level of strain are referred to using the subscript "cont $\epsilon$."

In comparing these two design approaches, two basic requirements are being met: first, that the strain in the structure at ultimate load be equal to the design ultimate strain; and secondly, that the strain at limit load be such that

damage of a given size does not propagate. It will be seen that both of these conditions are important and that either one can be critical, depending on damage size and design ultimate strain.

The thickness required to satisfy ultimate design strain is

$$t_u = N/E\epsilon_u \tag{7}$$

where

$N$ = ultimated load, lb/in.
$\epsilon_u$ = design ultimate strain

and the thickness required to prevent damage propagation is

$$t_d = \tfrac{2}{3}(N/E\epsilon_d) \tag{8}$$

where

$\epsilon_d$ = critical gross crack propagation strain

The thickness increase necessary to add damage survivability capability to a design can be expressed as the ratio

$$t_d/t_u = \tfrac{2}{3}(\epsilon_u/\epsilon_d) \tag{9}$$

Using a design ultimate strain of 4000 $\mu$ in./in. as a base point, this ratio for $[0°/\pm 45°/0°]_{ns}$ graphite-epoxy without crack arrester strips can be determined as a function of damage size using Eq. (9) and taking $\epsilon_d$ from the initial propagation curve of Fig. 3. This ratio is plotted in Fig. 8. Note that a structure which is sized for an ultimate strain of 4000 $\mu$ in./in. has an inherent capability to sustain, at limit load, damage up to about 1.2 in. It also is seen that this curve levels off at a value of 1.57, corresponding to the leveling off of the initial propagation curve in Fig. 3, indicating that to achieve damage tolerance using the brute force approach of adding thickness to keep the strains low requires a 57% increase in thickness (and weight) to accommodate large damage sizes.

Using the crack arrester approach several requirements must be met. First, since there is no control over where damage is inflicted, it must be assumed that it occurs directly on one of the arrester strips. This makes the arrester strip spacing effectively two-bays wide as opposed to the situation where the damage occurs midbay. There also can be a situation where damage equal in size to one bay width plus two strip widths could result in two strips being damaged and the effective spacing being three bays, and so on. These situations have been considered in these tradeoffs by assuming the worst-case positioning of damage for each damage size.

The second requirement is one of making the panel with crack arrest strips just as stiff as one without them, that is satisfying Eq. (7), so that the overall strain level is not increased. This requires increasing the thickness because the lower modulus of glass-epoxy decreases the effective modulus of the panel. This variation in effective modulus is shown in Fig. 9 as a function of arrester strip width and spacing.

Finally, even though crack propagation is permitted with crack arrester strips, it is contained locally, and the requirements for residual strength must be met as given by Fig. 3 for multibay panels in conjunction with Eq. (8).

Based on these considerations and the 4000 $\mu$ in./in. design ultimate strain, the thickness of a structure with crack arrester strips was determined using ¼-in. wide strips for two spacings, 1 in. and 8 in. The results are given in Fig. 8. For both spacings the curves are constant with damage size because the residual strain capability is equal to or exceeds the limit strain over the range of damage sizes considered, and so the only increase in thickness which is necessary is to offset the decrease in effective stiffness.

The horizontal portion of the solid curves are cutoffs, depending on design ultimate strain, and are indicative of the inherent damage resistance of a structure designed to that strain level.

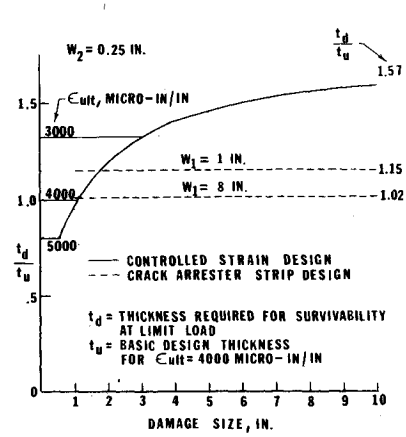


**Fig. 8 Comparison of crack arrester and controlled strain designs.**

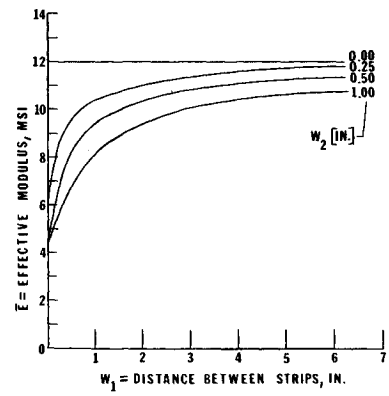


**Fig. 9 Stiffness of panels with crack arrester strips.**

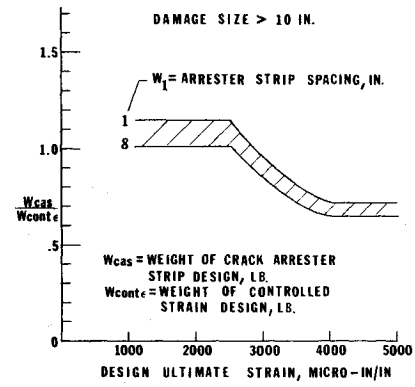


**Fig. 10 Effect of design strain level on crack arrester strip application.**

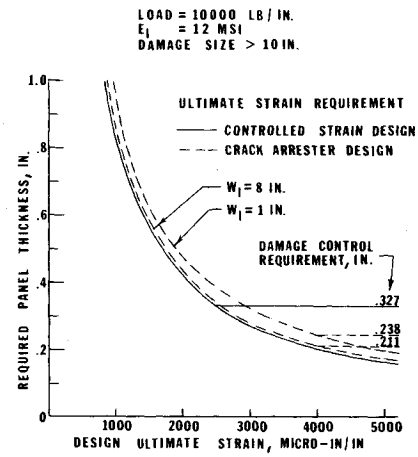


**Fig. 11 Example of thickness requirement variation.**

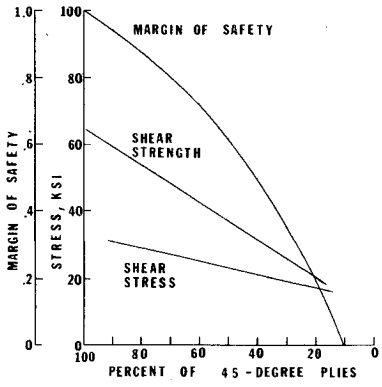


**Fig. 12 Effect of laminate configuration on residual strength.**

Although the specimen testing was done with ½-in. wide strips, these tradeoffs are based on the use of ¼-in. wide strips in order to show maximum weight saving potential. Since very little crack tip penetration into the arrester strips was experienced with the ½-in. width, it is felt that ¼-in. wide strips would be equally effective. Testing to confirm this is underway. The tradeoff conclusions given earlier would be equally valid for ½-in. wide strips, except that the thickness ratios for 1-in. and 8-in. spacings would be 1.28 and 1.06, respectively, instead of 1.15 and 1.02.

The importance of the results of this tradeoff is that crack arrester strips can be used to achieve survivability with much less weight than with a controlled strain design. For the ground rules, materials, and laminate configurations considered here the weight penalty is as little as 2%, compared to 57% for the alternate approach. It should be pointed out that weight increase is being equated to thickness increase in this discussion. Even though the glass-epoxy has a higher density than graphite-epoxy, the actual weight increase in the panel is negligible.

Consider next the effect that design ultimate strain has on this comparison. This is to say, if requirements other than damage survivability dictate lower or higher design ultimate strains, what impact would this have on the conclusions just reached? To explore this, the tradeoff was repeated using other ultimate strain values and considering large damage size, i.e., >10 in. The results are given in Fig. 10, showing the ratio of weight of the crack arrester design to the weight of the controlled strain design, again for two crack arrester strip spacings, as a function of ultimate design strain level.

Several important points are brought out by Fig. 10. It is seen that for design ultimate strains of less than 2550 $\mu$ in./in., crack arrester designs are heavier than controlled strain designs. This is because crack arrester strips are not needed at these ultimate strain levels, since the limit strain is low enough that the structure inherently can accommodate the damage. In the range from 2550 $\mu$ in./in. to 4000 $\mu$ in./in., crack arrester designs are lighter than controlled strain designs, by as much as 36% at the higher values. Above 4000 $\mu$ in./in. the weight saving remains a constant value of 36%. The reason for this is that above 4000 $\mu$ in./in. the weight of both designs is governed by the damage propagation requirement, Eq. (8), which for a given load and given damage size (and, therefore, a given critical strain) is a given thickness, which is independent of design ultimate strain. It also is seen that, in general, the 1-in. spaced crack arrester strip design is 10-15% heavier than the 8-in. spacing.

An example of this is given in Fig. 11 for load $N=10{,}000$ lb/in., $E_l=12\times10^6$ psi, and damage size greater than 10 in. For the controlled strain design and the two crack arrester designs the basic thickness required to satisfy the ultimate strain requirement decreases as ultimate design strain increases. Also, in all three cases, a particular thickness will prevent damage propagation for the limit load of 6667 lb/in., that thickness indicated by the horizontal cutoff lines, as determined by Eq. (8). It is seen clearly that for larger values of design ultimate strain the requirement for damage control sets the thickness, whereas for smaller design ultimate strains the thickness required to limit this ultimate strain is more than that required to prevent damage propagation. The difference between the ultimate strain thickness requirements for the controlled strain design and the crack arrester designs in Fig. 11 is due to the lower effective modulus of the latter, as previously discussed. Note also that, if the ordinates of the solid curve of Fig. 11 are divided by the ordinate of the dashed curves, the ratios are equal to the values given in Fig. 10 for $W_{CAS}/W_{\text{conte}}$.

Another area for investigation is the effect of laminate configuration. Since shear strength obviously has a major influence on residual strength, one way to increase this residual strength is to use a layup with more $\pm45°$ plies. A brief look at this has been taken and the results are given in Fig. 12 where it can be seen that increasing the percentage of 45° plies will increase shear stress, but also increase shear strength even more, resulting in a greater margin of safety against shear failure.

## Conclusions

As was stated in the introductory remarks of this paper, it is felt that the work presented here nearly completes the first phase of work on crack arrester strip design. It has been demonstrated that they successfully arrest propagating cracks in graphite-epoxy composites. Furthermore, the important failure modes which govern their behavior have been identified and investigated both analytically and experimentally. A limited design base for one material system has been generated with a relatively good degree of accuracy. Finally, tradeoff studies, using the experimentally developed data base, have indicated that the ability to sustain large damage sizes (~8-10 in.) can be built into an advanced composite structure using integral crack arrester strips with very small weight penalty (~2%).

Although this phase of work has demonstrated basic feasibility and usefulness of this design approach, much work remains to be done. Perhaps the most important aspect of this future work is the further characterization and improvement of the residual strength. The results given here, and in particular the tradeoff results, although indicating advantages to be had using crack arrester strips, are based on very limited residual strength testing.

Other questions which require investigation are fatigue and environmental effects, and the influence of initial damage not being midway between crack arrester strips. In all of the testing to date, no crack eccentricity has been used.

Although cost has not been directly addressed here, it is felt that any cost penalties associated with building crack arrester strips into a panel are very small. Prepregs already are being made which have glass strips in them, which eliminates the cutting and placing of separate glass strips as was done in fabricating the test specimens. Other than that, cost would be related almost directly to thickness and weight, so that where weight savings are shown it is expected that comparable cost savings would be realized. To truly evaluate cost, one would need to go a level or two beyond fabrication costs and consider the impact of increased aircraft survivability resulting from the incorporation of the arrester strips in a design.

## References

[1] Huang, S. L. and Hess, T. E., "A Hybrid Fuselage Design with Integral Crack Arresters," *3rd Conference on Fibrous Composites in Flight Vehicle Design*, NASA and USAF, Williamsburg, Va., Nov. 4-6, 1975.

[2] Eisenmann, J. R. and Kaminski, E. E., "Fracture Control for Composite Structures," Convair Aerospace Division Rept. ERR-FW-1341, Jan. 1972.

[3] Sendickyj, G. P., "Concepts for Crack Arrestment in Composites," *Fracture Mechanics of Composites*, American Society for Testing Materials, ASTM STP 593, 1975, pp. 215-226.